Molecular Biology of the Cell
Vol. 15, 4854–4865, November 2004

Megator, an Essential Coiled-Coil Protein that Localizes to the Putative Spindle Matrix during Mitosis in *Drosophila*

Hongying Qi,*† Uttama Rath,*† Dong Wang,* Ying-Zhi Xu,* Yun Ding,* Weiguo Zhang,* Melissa J. Blacketer,* Michael R. Paddy,‡ Jack Girton,* Jørgen Johansen,* and Kristen M. Johansen*§

*Department of Biochemistry, Biophysics, and Molecular Biology, Iowa State University, Ames, IA 50011; and ‡Section of Molecular and Cellular Biology, University of California at Davis, Davis, CA 95616

Submitted July 10, 2004; Revised August 24, 2004; Accepted August 25, 2004
Monitoring Editor: Joseph Gall

We have used immunocytochemistry and cross-immunoprecipitation analysis to demonstrate that Megator (Bx34 antigen), a Tpr ortholog in *Drosophila* with an extended coiled-coil domain, colocalizes with the putative spindle matrix proteins Skeletor and Chromator during mitosis. Analysis of P-element mutations in the *Megator* locus showed that Megator is an essential protein. During interphase Megator is localized to the nuclear rim and occupies the intranuclear space surrounding the chromosomes. However, during mitosis Megator reorganizes and aligns together with Skeletor and Chromator into a fusiform spindle structure. The Megator metaphase spindle persists in the absence of microtubule spindles, strongly implying that the existence of the Megator-defined spindle does not require polymerized microtubules. Deletion construct analysis in S2 cells indicates that the COOH-terminal part of Megator without the coiled-coil region was sufficient for both nuclear as well as spindle localization. In contrast, the NH_2-terminal coiled-coil region remains in the cytoplasm; however, we show that it is capable of assembling into spherical structures. On the basis of these findings we propose that the COOH-terminal domain of Megator functions as a targeting and localization domain, whereas the NH_2-terminal domain is responsible for forming polymers that may serve as a structural basis for the putative spindle matrix complex.

INTRODUCTION

Although much work has been directed toward understanding mitotic spindle apparatus structure and function, it is still unclear how mechanical forces are applied to pull the chromosomes to the spindle poles (Pickett-Heaps *et al.*, 1982; 1997; Scholey *et al.*, 2001). The involvement of a spindle matrix that can act as a stationary substrate to stabilize the spindle during force production, and microtubule sliding has long been proposed (Pickett-Heaps *et al.*, 1982; 1997); however, direct evidence for its existence has remained elusive (Scholey *et al.*, 2001; Wells, 2001; Bloom, 2002; Kapoor and Compton, 2002; Johansen and Johansen, 2002). Recently, a putative spindle matrix protein, Skeletor, was identified in *Drosophila* (Walker *et al.*, 2000). Skeletor is associated with chromosomes at interphase, but preceding microtubule spindle formation and nuclear lamina breakdown, it redistributes into a true fusiform spindle at prophase. During metaphase the Skeletor defined spindle and the microtubule spindles are coaligned and when embryos are treated with nocodazole to disassemble microtubules, the Skeletor spindle persists (Walker *et al.*, 2000). Thus, many of the features of the Skeletor defined spindle are consistent with the spindle matrix hypothesis. Using a yeast two-hybrid screen with Skeletor sequence as bait Rath *et al.* (2004) identified another potential component of a spindle matrix, Chromator, that interacts directly with Skeletor. Chromator contains a chromodomain and colocalizes with Skeletor on the chromosomes at interphase as well as to the Skeletor-defined spindle during metaphase. Furthermore, functional assays using P-element insertion mutants and RNAi in S2 cells suggest that Chromator is an essential protein that affects spindle function and chromosome segregation (Rath *et al.*, 2004).

The above findings supports the hypothesis that Skeletor and Chromator are members of a macromolecular spindle matrix complex constituted by several nuclear components (Walker *et al.*, 2000; Rath *et al.*, 2004). However, for a spindle matrix to form independently or to form a structural scaffold aligned with the microtubule spindle, one or more of its molecular components would be predicted to have the ability to form polymers. Neither Skeletor nor Chromator appears to contain molecular motifs with such properties. In this study we report the identification of another molecular component that localizes to the putative spindle matrix and is a candidate to play such a structural role. The mAb Bx34 was previously shown to recognize a 260-kDa protein with a large NH_2-terminal coiled-coil domain and a shorter COOH-terminal acidic region that shows overall structural and sequence similarity to the mammalian nuclear pore complex Tpr protein (Zimowska *et al.*, 1997). Zimowska *et al.* (1997) showed that the Bx34 antigen during interphase was localized to the nuclear rim as well as occupying the intranuclear space surrounding the chromosomes. Here we show using immunocytochemistry and analysis of P-element mutations that the Bx34 antigen is an essential protein that colocalizes with Skeletor and Chromator to the putative spindle matrix as it is defined by these proteins during

Article published online ahead of print. Mol. Biol. Cell 10.1091/mbc.E04–07–0579. Article and publication date are available at www.molbiolcell.org/cgi/doi/10.1091/mbc.E04–07–0579.

† These authors contributed equally to this work.

§ Corresponding author. E-mail address: kristen@iastate.edu.

mitosis. Furthermore, based on the presence of the large coiled-coil domain, we propose the Bx34 antigen may serve as a structural component of the spindle matrix and have named the protein Megator.

MATERIALS AND METHODS

Drosophila *Stocks*

Fly stocks were maintained according to standard protocols (Roberts, 1986). Oregon-R or Canton-S was used for wild-type preparations. The *y*^{1} *w*^{67c23}; *P{w*$^{+mC}$ *= lacW}l(2)k03905*^{k03905}*/CyO* line was obtained from the Bloomington Stock Center and was originally part of the István Kiss collection (Trk *et al.*, 1993). To facilitate identification of homozygous mutant Megator embryos, *P{w*$^{+mC}$ *= lacW}l(2)k03905*^{k03905} was balanced over one of two different green fluorescent protein (GFP)-tagged *CyO* balancers obtained from the Bloomington Stock Center line: *w*; In(2LR)nocScorv9R, b1/CyO, P{w*$^{+mC}$ *= Act-GFP}JMR1* or *CyO, P{w*$^{+mC}$ *= GAL4-Kr. C}DC3, P{w*$^{+mC}$ *= UAS-GFP. S65T}DC7*. Control antibody labelings were performed on embryos from these lines.

Antibodies

Residues 1433–1703 of the predicted Megator protein were subcloned using standard techniques (Sambrook *et al.*, 1989) into the pGEX-4T-1 vector (Amersham Pharmacia Biotech, Piscataway, NJ) to generate the construct GST-270. The correct orientation and reading frame of the insert was verified by sequencing. GST-270 fusion protein was expressed in XL1-Blue cells (Stratagene, La Jolla, CA) and purified over a glutathione agarose column (Sigma-Aldrich, St. Louis, MO), according to the pGEX manufacturer's instructions (Amersham Pharmacia Biotech). The mAbs 12F10 and 11E10 were generated by injection of 50 μg of GST-270 into BALB/c mice at 21-d intervals. After the third boost, mouse spleen cells were fused with Sp2 myeloma cells, and monospecific hybridoma lines were established using standard procedures (Harlow and Lane, 1988). The mAb 12F10 is of the IgG1 subtype. All procedures for mAb production were performed by the Iowa State University Hybridoma Facility. The anti-Skeletor mAb 1A1 (Walker *et al.*, 2000), anti-Chromator mAbs 6H11 and 12H9 (Rath *et al.*, 2004), anti-Bx34 antigen mAb Bx34 and polyclonal antiserum (Zimowska *et al.*, 1997), and antilamin mAb ADL195 (Klapper *et al.*, 1997) have been previously described. mAb ADL195 was obtained from the Developmental Studies Hybridoma Bank at University of Iowa. Anti-α-tubulin (mouse mAbs of the IgG1 [Sigma-Aldrich] and IgM [Abcam, Cambridge, United Kingdom] subtypes and a rat mAb [Abcam]) as well as anti-V5 antibody (Invitrogen, Carlsbad, CA) were obtained from commercial sources.

Biochemical Analysis

SDS-PAGE and Immunoblotting. SDS-PAGE was performed according to standard procedures (Laemmli, 1970). Electroblot transfer was performed as in Towbin *et al.* (1979) with transfer buffer containing 20% methanol and in most cases including 0.04% SDS. For these experiments we used the Bio-Rad Mini PROTEAN II system, electroblotting to 0.2 μm nitrocellulose, and using anti-mouse HRP-conjugated secondary antibody (Bio-Rad, Richmond, CA; 1:3000) for visualization of primary antibody diluted 1:1000 in Blotto. The signal was visualized using chemiluminescent detection methods (ECL kit, Amersham, Long Beach, CA). The immunoblots were digitized using a flatbed scanner (Epson Expression 1680). For quantification of immunolabeling, digital images of exposures of immunoblots on Biomax ML film (Eastman Kodak, Rochester, NY) were analyzed using the ImageJ software as previously described (Wang *et al.*, 2001). In these images the grayscale was adjusted such that only a few pixels in the wild-type lanes were saturated. The area of each band was traced using the outline tool, and the average pixel value determined. Homozygous mutant Megator embryos selected from *P{w*$^{+mC}$ *= lacW}l(2)k03905*^{k03905}*/CyO, P{w*$^{+mC}$ *= Act-GFP}JMR1* parents and identified by virtue of lack of GFP signal were obtained from 15–20 h embryo collections. Heterozygous *l(2)k03905/CyO* and *CyO/CyO* embryos from the same embryo collection served as a reference for the reduction in Megator protein levels in homozygous embryos. Similar experiments were performed using *P{w*$^{+mC}$ *= lacW}l(2)k03905*^{k03905}*/CyO, P{w*$^{+mC}$ *= GAL4-Kr. C}DC3*, and *P{w*$^{+mC}$ *= UAS-GFP. S65T}DC7* parents to minimize maternal GFP levels. Quantification of labeling on Western blots of *l(2)k03905* mutant embryos were determined as a percentage relative to the level determined for control embryos using tubulin levels as a loading control. In RNAi experiments Megator levels in experimental and control S2 cell cultures were normalized using tubulin loading controls for each sample.

Immunoprecipitation Assays. For coimmunoprecipitation experiments, anti-Megator or anti-Chromator antibodies were bound to protein G beads (Sigma) as follows: 10 μl of mAb 12F10 ascites or 100 μl of mAb 12H9 supernatant was bound to 30 μl protein G-Sepharose beads (Sigma) for 2.5 h at 4°C on a rotating wheel in 50 μl immunoprecipitation (ip) buffer. The appropriate antibody-coupled beads or beads only were incubated overnight at 4°C with 200 μl of 0–3 h embryonic lysate on a rotating wheel. Beads were washed three times for 10 min each with 1 ml of ip buffer with low-speed pelleting of beads between washes. The resulting bead-bound immunocomplexes were analyzed by SDS-PAGE and Western blotting according to standard techniques (Harlow and Lane, 1988) using mAb 6H11 to detect Chromator and mAb 12F10 to detect Megator.

Immunohistochemistry

Antibody labelings of 0–3-h embryos were performed as previously described (Johansen *et al.*, 1996; Johansen and Johansen, 2003). The embryos were dechorionated in a 50% Chlorox solution, washed with 0.7 M NaCl/0.2% Triton X-100 and fixed in a 1:1 heptane:fixative mixture for 20 min with vigorous shaking at room temperature. The fixative was either 4% paraformaldehyde in phosphate-buffered saline (PBS) or Bouin's fluid (0.66% picric acid, 9.5% formalin, 4.7% acetic acid). Vitelline membranes were then removed by shaking embryos in heptane-methanol (Mitchison and Sedat, 1983) at room temperature for 30 s. S2 cells were affixed onto poly-L-lysine–coated coverslips and fixed with Bouin's fluid for 10 min at 24°C and methanol for 5 min at −20°C. The cells on the coverslips were permeabilized with PBS containing 0.5% Triton X-100 and incubated with diluted primary antibody in PBS containing 0.1% Triton X-100, 0.1% sodium azide, and 1% normal goat serum for 1.5 h. Double and triple labelings employing epifluorescence were performed using various combinations of antibodies against Megator (mAb 12F10, IgG1), Chromator (mAb 6H11, IgG1), Skeletor (mAb 1A1, IgM), anti-α-tubulin mouse IgG1 or IgM antibody, anti-α-tubulin rat IgG2a, antilamin antibody (IgM), V5-antibody (IgG2a), and Hoechst to visualize the DNA. The appropriate species and isotype specific Texas Red-, TRITC-, and FITC-conjugated secondary antibodies (Cappel/ICN, Southern Biotechnology, Birmingham, AL) were used (1:200 dilution) to visualize primary antibody labeling. Confocal microscopy was performed with a Leica confocal TCS NT microscope system (Deerfield, IL) equipped with separate argon-UV, argon, and krypton lasers and the appropriate filter sets for Hoechst, FITC, Texas Red, and TRITC imaging. A separate series of confocal images for each fluorophor of double-labeled preparations were obtained simultaneously with z-intervals of typically 0.5 μm using a PL APO 100×/1.40–0.70 oil objective. A maximum projection image for each of the image stacks was obtained using the ImageJ software. In some cases individual slices or projection images from only two to three slices were obtained. Images were imported into Photoshop where they were pseudocolored, image processed, and merged (Adobe Systems, San Jose, CA). In some images nonlinear adjustments were made for optimal visualization especially of Hoechst labelings of nuclei and chromosomes. Polytene chromosome squash preparations from late third instar larvae were immunostained by the Skeletor antibody mAb 1A1 and Megator antibody mAb 12F10, essentially as previously described by Zink and Paro (1989), Jin *et al.* (1999), and Wang *et al.* (2001).

Microtubule Depolymerization Experiments

Dechorionated embryos from 0–2.5-h collections were added to heptane containing 10 μM nocodazole (Sigma-Aldrich) and shaken for 1.5 min, before adding fixative and incubating for an additional 20 min. Cold-treated embryos were dechorionated on ice for 2 min and incubated for 1 min with prechilled heptane. Prechilled Bouin's fluid was then added to the heptane layer, shaken for 30 s, and rotated at 4°C for 20 min. Immunolabeling was performed as described above.

Expression of Megator Constructs in Transfected S2 Cells

A full-length Megator (2346 aa) construct, a NH_2-terminal domain construct of Megator from residue 1–1431 containing 87% of the coiled-coil region, and a COOH-terminal domain construct of Megator from residue 1758–2346 were cloned into the pMT/V5-HisB vector (Invitrogen) with in-frame V5 tags at the COOH-termini using standard methods (Sambrook *et al.*, 1989). Similarly, a middle construct from residue 1432–1709 was subcloned into the pMT/V5-HisA vector with an in-frame V5-tag at the COOH-terminus. The fidelity of all constructs was verified by sequencing at the Iowa State University Sequencing facility.

Drosophila Schneider 2 (S2) cells were cultured in Shields and Sang M3 insect medium (Sigma) supplemented with 10% fetal or newborn bovine serum, antibiotic/antimycotic solution, and L-glutamine (Life Technologies/BRL/Life Technologies) at 25°C. The S2 cells were transfected with different Megator subclones using a calcium phosphate transfection kit (Invitrogen), and expression was induced by 0.5 mM $CuSO_4$. Cells expressing Megator constructs were harvested 12–24 h after induction and affixed onto poly-L-lysine–coated coverslips for immunostaining and Hoechst labeling.

RNAi Interference

dsRNAi in S2 cells was performed according to Clemens *et al.* (2000). A 784-base pair fragment encoding sequence from the coiled-coil region of Megator cDNA was PCR amplified and used as template for in vitro transcription using the Megascript RNAi kit (Ambion, Austin, TX). Synthesized dsRNA, 40 μg, was added to 1×10^6 cells in six-well cell culture plates.

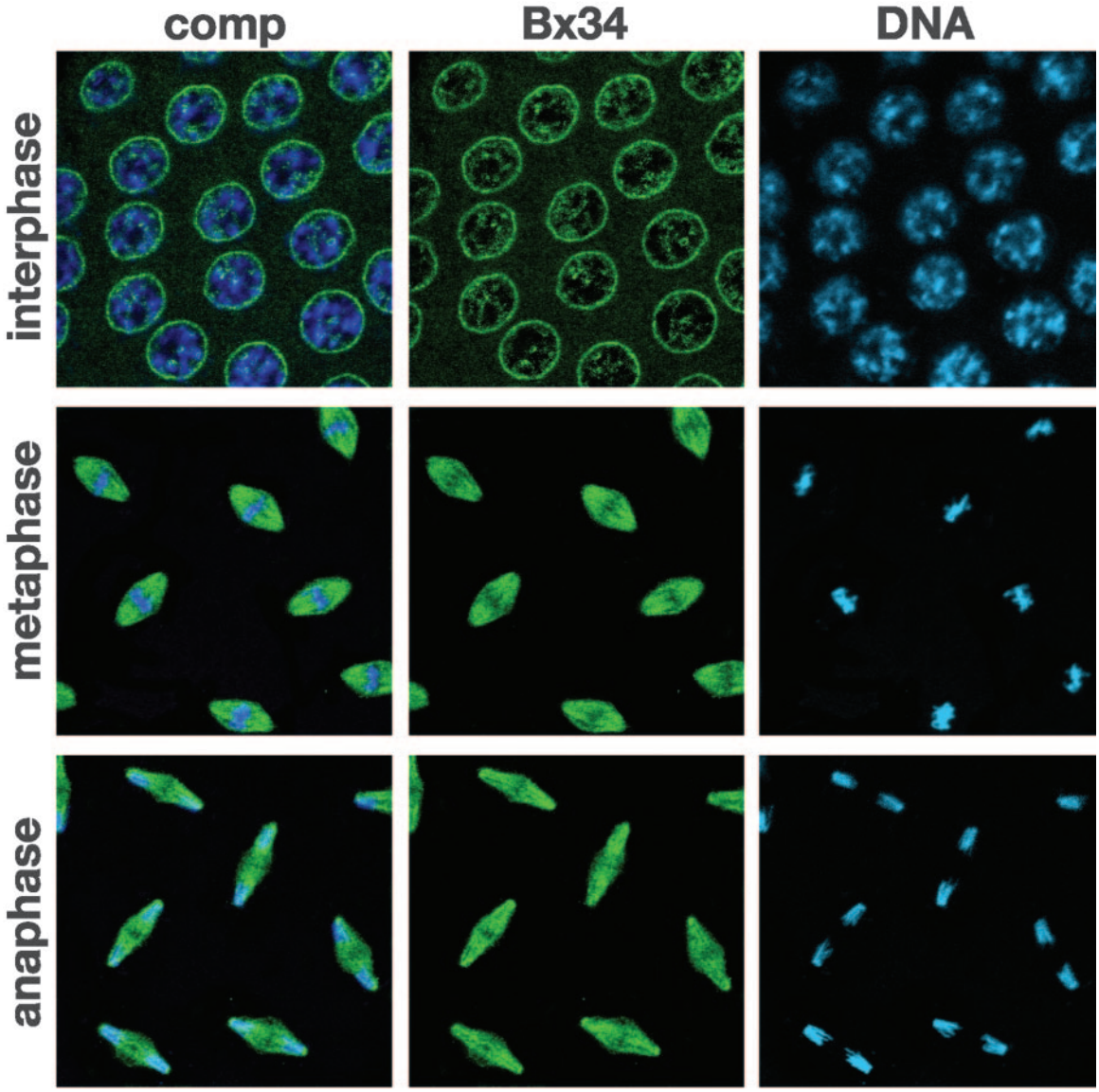

Figure 1. Syncytial *Drosophila* embryo nuclei labeled by mAb Bx34 and Hoechst from various stages of the cell cycle (inter-, meta-, and anaphase). The labeling by mAb Bx34 is shown in green and the labeling of DNA by Hoechst in blue. The composite (comp) images of the stainings are to the left. At interphase the Bx34 antibody labels the nuclear rim together with interior nuclear labeling. At meta- and anaphase the Bx34 antibody labels a spindle-like structure. All images in these panels are from confocal sections.

Control dsRNAi experiments were performed identically except pBluescript vector sequence (800 base pairs) was used as template. The dsRNA-treated S2 cells were incubated for 120 h and then processed for immunostaining and immunoblotting. For immunoblotting 10^5 cells were harvested, resuspended in 50 μl of S2 cell lysis buffer (50 mM Tris-HCl, pH 7.8, 150 mM NaCl, and 1% Nonidet P-40), boiled, and analyzed by SDS-PAGE and Western blotting with anti-Megator antibody (mAb 12F10) and anti-α tubulin antibody. The mitotic index defined as the number of cells in metaphase and anaphase as a percentage of total cell number were compared between experimental and control S2 cell cultures. At least 500 cells were examined in each individual experiment (range: 500-2500 cells).

Analysis of P-element Mutants

PCR Mapping. The insertion site flanking sequence provided by the Berkeley *Drosophila* Genome Project for the *P{w*$^{+mC}$ *= lacW}l(2)k03905*^{k03905} element (Accession no. AQ025733) placed the P-element insertion near the transcription start site for the Megator gene. By designing several sets of nested forward and reverse primers from genomic sequence encompassing this region, we performed PCR from mutant flies as previously described (Preston and Engels, 1996). PCR fragments were subcloned and sequenced according to standard protocols (Sambrook *et al.*, 1989).

Viability Assays. To determine the viability of Megator mutants, we analyzed the offspring from crosses of *l(2)k03905/CyO, P{w*$^{+mC}$ *= Act-GFP}JMR1* parents in which the balancer chromosome is labeled with GFP, allowing for the identification of homozygous *l(2)k03905/l(2)k03905* embryos and larvae. For these assays eggs were collected on standard yeasted agar plates and incubated at 21°C. No homozygous *l(2)k03905/l(2)k03905* larvae were found among 200 third instar larvae examined from such crosses, and among 300 embryos only one homozygous *l(2)k03905/l(2)k03905* first instar larvae emerged.

P-element Excision. The P element of *y*^{1} *w*^{67c23}*; P{w*$^{+mC}$ *= lacW}l(2)k03905*^{k03905}*/CyO* was mobilized by a Δ 2–3 transposase source (*y*^{1} *w***; CyO, H{w*$^{+mC}$ *= P*Δ *2–3}HoP2.1/Bc*^{1}*Egfr*^{E1}; Robertson *et al.*, 1988). Several fly lines in which the P element had been excised were identified by their white eye color. Three precise excisions were confirmed by PCR analysis using primers corresponding to the P element and/or the genomic sequences flanking it. DNA isolation from single flies and PCR reactions were performed as

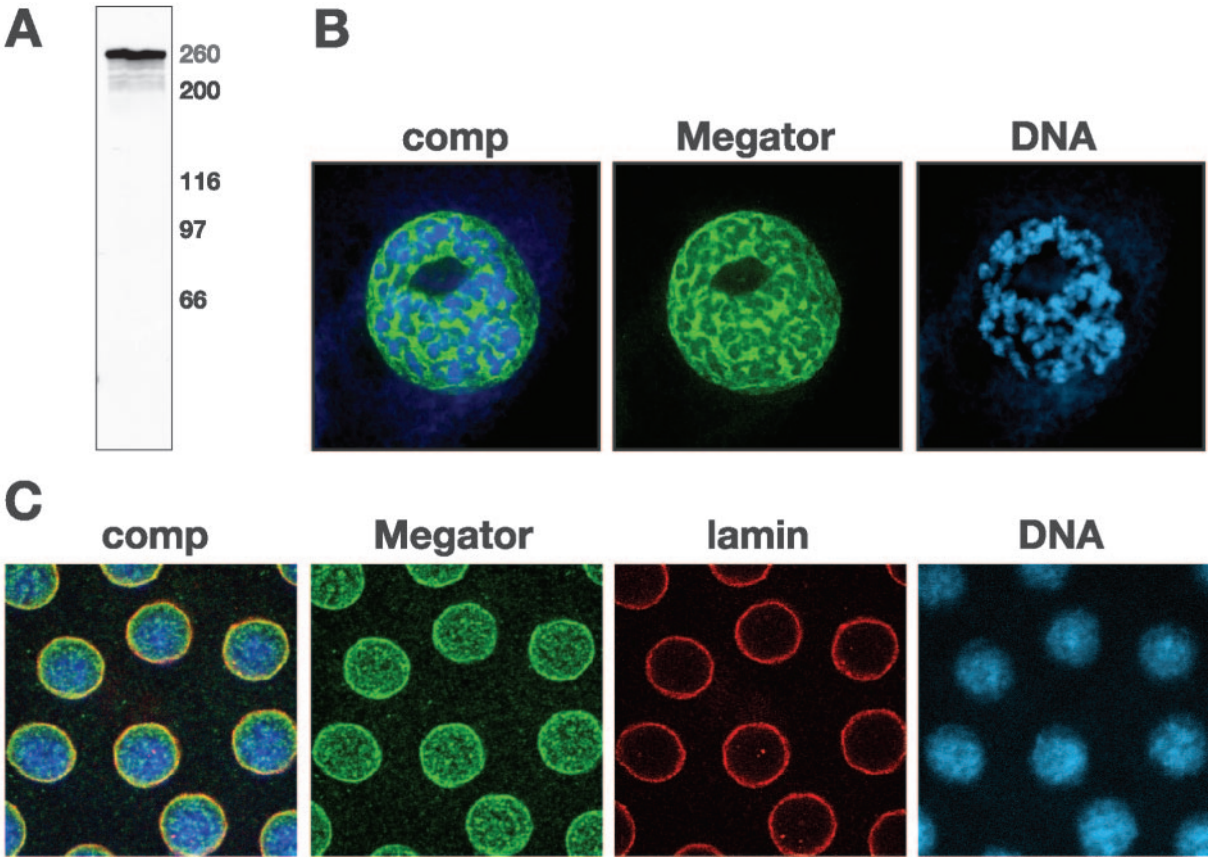

Figure 2. Immunoblot and interphase nuclear labeling of the Megator mAb 12F10. (A) Western blot analysis of *Drosophila* embryonic protein extract shows that mAb 12F10 recognizes Megator protein as a 260-kDa band. The migration of molecular-weight markers are indicated to the right in black numerals. (B) Larval polytene nucleus labeled with mAb 12F10 (green) and Hoechst (blue). The composite image (comp) clearly indicates that the Megator labeling by mAb 12F10 surrounds the chromosomal DNA labeled by Hoechst. (C) Triple labelings using mAb 12F10 to visualize Megator (green), antilamin antibody to visualize the nuclear lamina (red), and Hoechst to visualize the DNA (blue) of interphase syncytial embryonic nuclei. The composite image (comp) shows that Megator and lamin labeling overlaps at the nuclear rim (yellow color), whereas interior nuclear Megator is interspersed with the DNA labeling of Hoechst. The images are from confocal sections.

described in Preston and Engels (1996). The precise excision lines were further analyzed for viability as described above and for restoration of Megator protein levels by immunoblotting. Protein extracts were prepared by homogenizing adult flies in IP buffer. Homozygous excised *l(2)k03905* flies were identified by the absence of the *Curly* marker. Proteins were separated on SDS-PAGE and analyzed by Western blotting with anti-Megator antibody (mAb 12F10) and anti-α tubulin antibody.

RESULTS

The Putative Spindle Matrix Protein Skeletor Colocalizes with the Bx34 Antigen (Megator) during Mitosis

In a search for candidate proteins that potentially could interact with the putative spindle matrix, we conducted labeling studies with the Bx34 mAb (Zimowska *et al.*, 1997). The Bx34 antigen (Megator) previously was found to be localized to the nuclear rim and to the nuclear extrachromosomal space during interphase; however, considerable Bx34 immunoreactivity was also reported to be present around the metaphase plate during mitosis, although the nature of this labeling was not resolved (Zimowska *et al.*, 1997). Similar labeling around the metaphase plate was also observed by Frasch *et al.* (1986) with several other *Drosophila* mAbs. For these reasons we revisited the issue of mAb Bx34's labeling during the cell cycle in syncytial *Drosophila* embryos fixed with Bouin's fluid, a precipitative fixative characterized by its rapid penetration and efficient fixation of nuclear proteins (Johansen and Johansen, 2003). As illustrated in Figure 1 the Bx34 mAb in addition to its characteristic interphase staining pattern also labeled what appeared to be fusiform spindle structures at meta- and anaphase. We observed this distribution of Megator both in Bouin's fluid and PFA fixed preparations as well as with a polyclonal antiserum made toward a synthetic peptide based on Megator's amino acid sequence (Zimowska *et al.*, 1997). Although the spindle-like labeling of the Bx34 mAb was intriguing and suggested a potential colocalization with the putative spindle matrix proteins the antibody was insufficiently robust for double labeling studies. We therefore generated new Megator mAbs, 12F10 and 11E10, against a GST fusion protein containing residues 1433–1703 of the Megator protein. Both mAbs label a single protein band of ~260 kDa on immunoblots of S2 cell protein extracts consistent with the predicted molecular mass of Megator of 262 kDa (Figure 2A) and recapitulate the reported interphase distribution of Megator at interphase. This is shown for polytene nuclei in Figure 2B, where the Megator labeling surrounds the chromosomes labeled with Hoechst and in confocal sections of embryonic syncytial nuclei in Figure 2C where the nuclear rim labeling coincides with that of lamin antibody. We subsequently

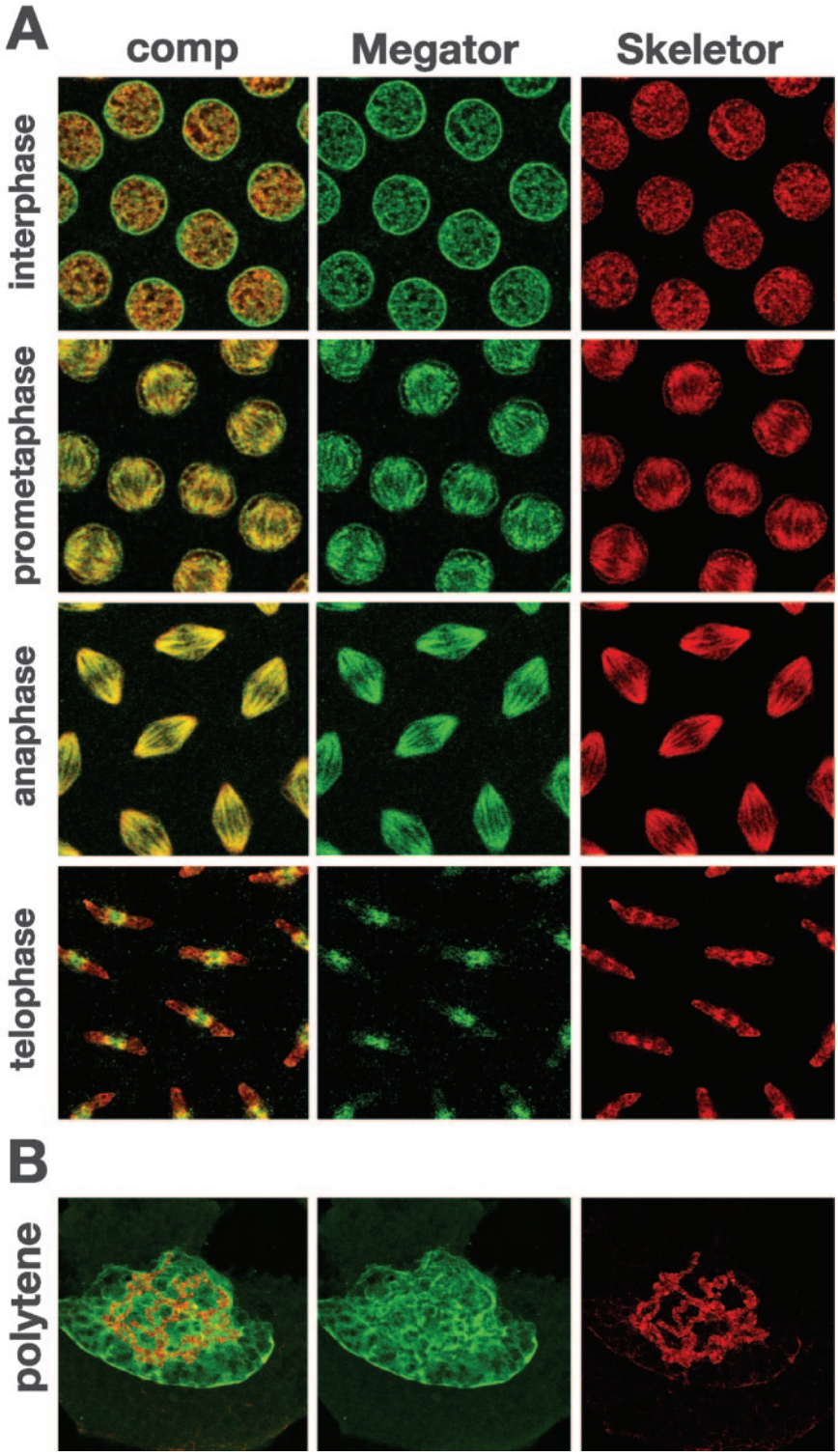

Figure 3. The dynamic redistribution of Megator relative to the putative spindle matrix protein Skeletor during the cell cycle. The images are from double labelings of Megator with mAb 12F10 (green) and Skeletor with mAb 1A1 (red). The composite images (comp) are shown to the left. (A) At interphase Skeletor and Megator labeling are intermingled in the nuclear interior, whereas Megator labeling is prominent at the nuclear rim. During prometa- and anaphase the composite images (comp) show extensive overlap between Megator and Skeletor labeling as indicated by the predominantly yellow color. At telophase where Skeletor begins to redistribute back to the chromosomes, Megator appears to be preferentially localized to the spindle midbody. The images are from confocal sections of syncytial embryonic nuclei. (B) Light squash of a larval polytene nucleus, where Skeletor localized on the chromosomes are surrounded by Megator labeling.

used mAb 12F10 (IgG1) to perform double labeling studies with the Skeletor antibody 1A1 (IgM) on fixed syncytial blastoderm embryos at different stages of mitosis (Figure 3). Figure 3A shows that although Megator and Skeletor labeling are intermingled in the nuclear interior, only Megator staining is prominent at the nuclear rim. Although embryonic interphase nuclei do not afford sufficient resolution to determine whether Skeletor and Megator labeling are separate in the nuclear interior, this can be clearly demonstrated in light squashes of polytene salivary gland nuclei where Skeletor is localized on the chromosomes that are surrounded by Megator labeling (Figure 3B). However, as mitosis commences Megator reorganizes during prophase into a fusiform spindle structure the pattern of which at prometaphase and anaphase appears identical to that of the putative spindle matrix protein Skeletor (Figure 3A). At telo-

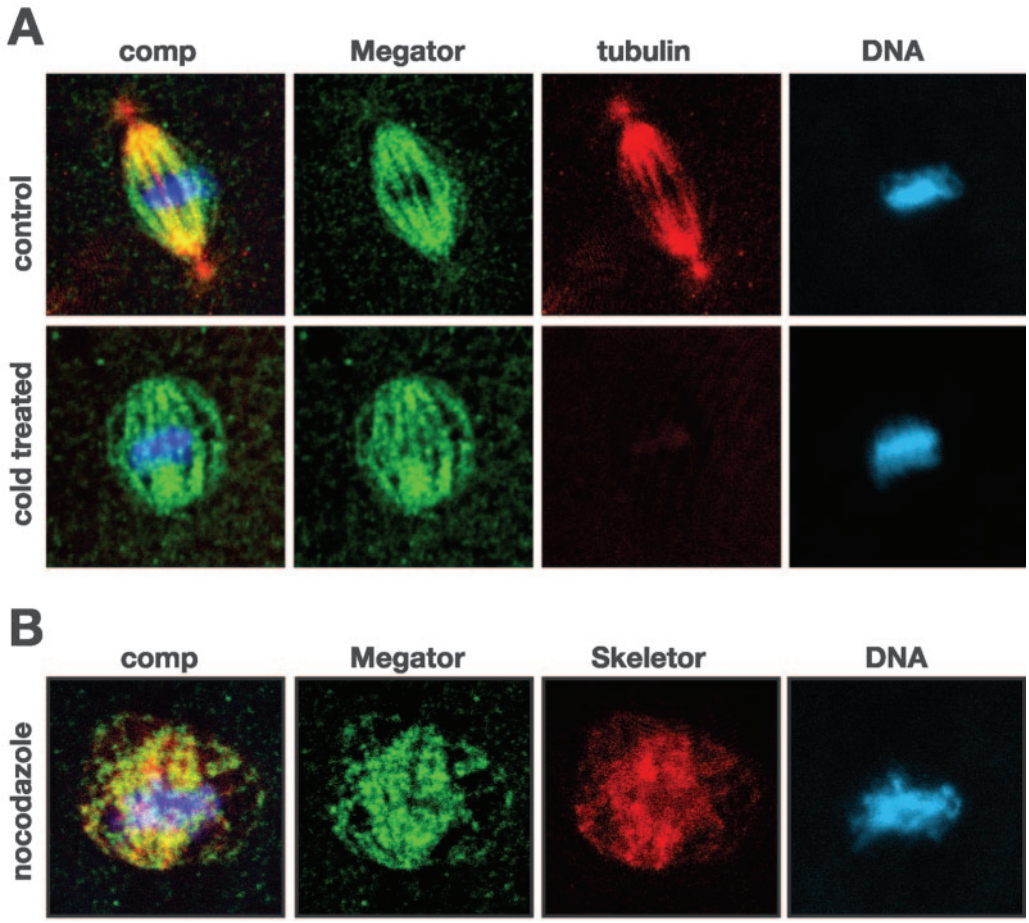

Figure 4. Nuclei from cold- or nocodazole-treated embryos at metaphase. (A) Control (top panel) and cold-treated (bottom panel) embryos triple-labeled with mAb 12F10 (green), rat α-tubulin antibody (red), and Hoechst (DNA in blue). In the cold-treated embryo microtubule spindles have completely depolymerized, as indicated by the absence of microtubule labeling. The mAb 12F10 labeled spindle (green) is still intact, demonstrating that this structure persists independently of the microtubule spindle. (B) Triple-labeling with mAb 12F10 (Megator in green), mAb 1A1 (Skeletor in red), and Hoechst (DNA in blue) from an embryo where microtubules were depolymerized with nocodazole. Both Megator and Skeletor labeling are still present and show extensive colocalization (yellow color in the composite [comp] image). All images are from confocal sections.

phase Skeletor begins to redistribute back to the decondensing chromosomes, whereas at this stage the majority of Megator is localized to the spindle midbody (Figure 3A).

To address the relationship between the Megator and microtubule spindles, we conducted triple-labeling studies in embryos where microtubules were disassembled by either nocodazole or cold treatment as previously described (Walker *et al.*, 2000). Figure 4A shows an image of a Megator spindle from a cold-treated embryo arrested at metaphase (bottom panel) compared with a control labeling (top panel). In the control labeling the Megator-defined spindle and the microtubule spindle are coaligned (Figure 4A, top panel). In contrast, after cold treatment there was no detectable tubulin antibody labeling indicating complete disassembly of the microtubules (Figure 4A, bottom panel). However, even in the absence of microtubule spindles, the Megator spindle remains intact implying that the existence of the Megator spindle does not require polymerized microtubules. Furthermore, under such depolymerized tubulin conditions both Megator and Skeletor spindle labeling are present and showing extensive colocalization (Figure 4B). This suggests that both Megator and Skeletor may be contributing to the formation of a spindle-like structure, the integrity of which is largely independent of microtubules.

The spindle localization of Megator is not restricted to the early embryonic cycles of nuclear division that lack the normal cell cycle checkpoints. We analyzed Megator distribution in the S2 cell line, which is a cell line that was originally derived from later stage embryonic cells (~16 h). In these cells, Megator shows a similar distribution pattern to that of syncytial blastoderm embryos (Figure 5). At interphase Megator is present in the nuclear interior and colocalizes with lamin at the nuclear rim (Figure 5A) whereas at metaphase Megator and Skeletor are colocalized at a spindle-like structure distinct from the chromosomes congregated at the metaphase plate (Figure 5B).

Megator Molecularly Interacts with the Putative Spindle Matrix Complex

To address whether Megator may interact with the putative Skeletor/Chromator spindle matrix complex we performed coimmunoprecipitation experiments designed to test for molecular interactions. For these experiments proteins were extracted from *Drosophila* embryos, immunoprecipitated with Megator or Chromator antibody, fractionated on SDS-PAGE after the immunoprecipitation, immunoblotted, and probed with antibody to Chromator and Megator, respectively. Figure 6A shows such an immunoprecipitation experiment where Chromator antibody coimmunoprecipitated a 260-kDa protein that is detected by Megator antibody on Western blots. Western blot analysis also confirms that this band comigrates with Megator protein from total embryo lysate or from Megator antibody immunoprecipitation samples. In the converse experiment the immunoprecipitate of Megator antibody contained a 130-kDa band detected by Chromator antibody that was also present in the lysate and in the Chromator immunoprecipitate sample (Figure 6B). This band was not present in lanes where immunobeads only were used for the immunoprecipitation (Figure 6, A

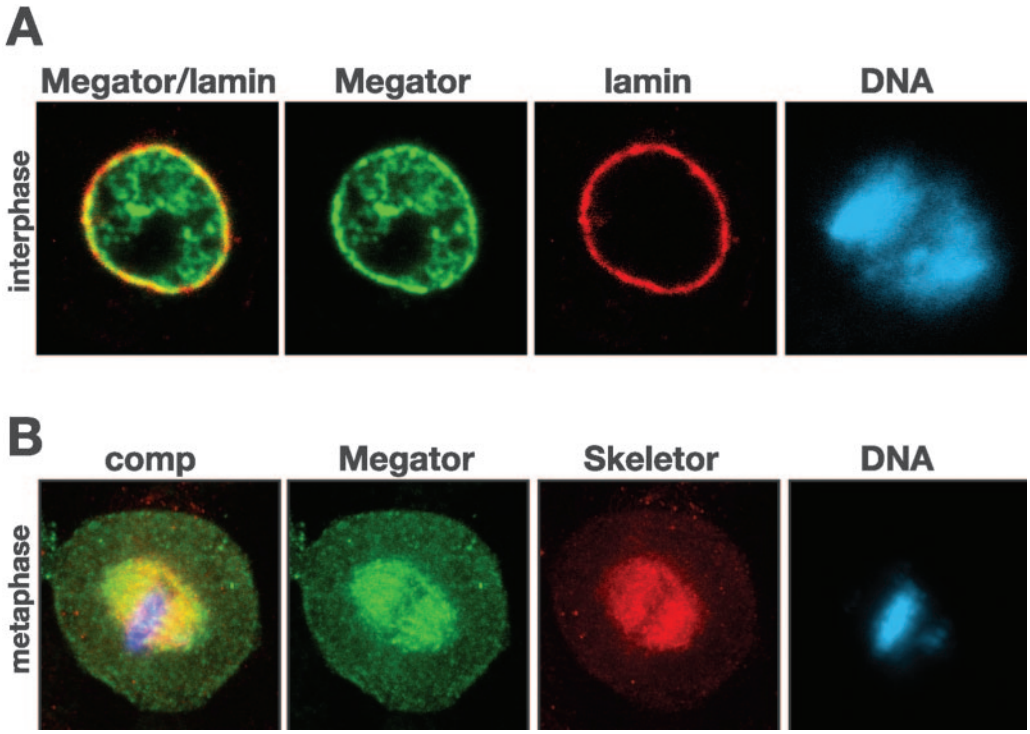

Figure 5. Nuclear localization of Megator in S2 cells. (A) Interphase nucleus labeled with mAb 12F10 (Megator in green), lamin antibody (red), and Hoechst (DNA in blue). The composite image (Megator/lamin) shows considerable overlap (yellow color) between Megator and lamin at the nuclear rim, whereas only Megator is detected in the nuclear interior. (B) Metaphase cell labeled with mAb 12F10 (Megator in green), mAb 1A1 (Skeletor in red), and Hoechst (DNA in blue). Megator and Skeletor labeling show extensive overlap (yellow color in the composite image [comp]) at the Skeletor defined spindle. All images are from confocal sections.

and B). These results provide evidence that Chromator and Megator are present in the same protein complex.

Megator Is an Essential Gene

Megator has been previously cloned and sequenced and encodes a large 2346 amino acid protein of 262 kDa in which the NH_2-terminal 70% is predicted to form an extended coiled-coil region while the COOH-terminal 30% is unstructured and acidic (Zimowska *et al.*, 1997; Figure 7A). It contains a putative nuclear localization signal (NLS) in the COOH-terminal part (Figure 7A). By PCR mapping and sequencing we determined that the P-element present in the *l(2)k03905* line (Spradling *et al.*, 1999) is inserted at the start of the published cDNA of Megator (Zimowska *et al.*, 1997) at position + 1 (Figure 7A). This insertion event also resulted in a 9-base pair duplication including 8 base pairs of upstream genomic sequence and a duplicated +1 residue. The site and nature of the insertion suggests that a functional Megator transcript is not likely to be made from the mutant gene and thus this insertion may represent a null mutation. To determine the viability of Megator mutants we analyzed the offspring from crosses of *l(2)k03905/CyO, P{w*$^{+mC}$ *= Act-GFP}JMR1* parents in which the balancer chromosome is labeled with GFP allowing for the identification of homozygous *l(2)k03905/l(2)k03905* embryos and larvae. No homozygous *l(2)k03905/l(2)k03905* larvae were found among 200 third instar larvae examined from such crosses and among 300 embryos only one homozygous *l(2)k03905/l(2)k03905* first instar larvae emerged. This suggests that the Megator protein is essential and that the lethality caused by the P-element mutation largely occurs during embryonic development as maternal stores are exhausted. Consistent with this we find that Western blots (Figure 7B) of homozygous 15–20 h *l(2)k03905* mutant Megator embryos show decreased Megator protein levels of only 28.5 ± 7.6% (n = 4) that of Megator levels in *l(2)k03905/CyO* and *CyO/CyO* embryos from the same embryo collection. We quantified this difference by determining the average pixel density of mAb Bx34 immunoblot staining of equal numbers of homozygous *l(2)k03905* mutant Megator embryos and control embryos. The remaining low level of Megator protein observed in the homozygous mutant is likely due to residual maternal stores.

In a recent study, it was found that in a significant percentage of lethal mutant lines carrying characterized P insertions, the lethal mutation was not directly associated with the P insertion event itself (Bellotto *et al.*, 2002). For this reason it was essential to confirm that the P insertion is the source of lethality for the *l(2)k03905* allele. To address this concern, we screened for precise excision events by introducing the Δ2–3 transposase to mobilize the transposon and then selecting for loss of the mini-white marker that is carried by the P-element. Stocks established from such flies were then analyzed by PCR to characterize the nature of the excision event to identify those lines with precise excisions of the P element. Test crosses of such lines demonstrated that the precise excision of the P element restored Megator expression and viability to flies that were homozygous for the second chromosome that had previously carried the *l(2)k03905* insertion (unpublished data). That precise excision of the *l(2)k03905* P element in three independent lines restores Megator expression and viability supports that the lethality observed in the *l(2)k03905* mutant line was directly due to the insertion of the P element in the *Megator* region.

Functional Consequences of Reduced Megator Protein Levels

The cross immunoprecipitation experiments and the immunolabeling results are consistent with that Megator and Chromator are present in the same macromolecular complex during mitosis. This suggests that Megator has the potential to play a functional role in proper cell division. Unfortunately, this hypothesis cannot be tested in homozygous *l(2)k03905* early embryos due to the presence of maternally

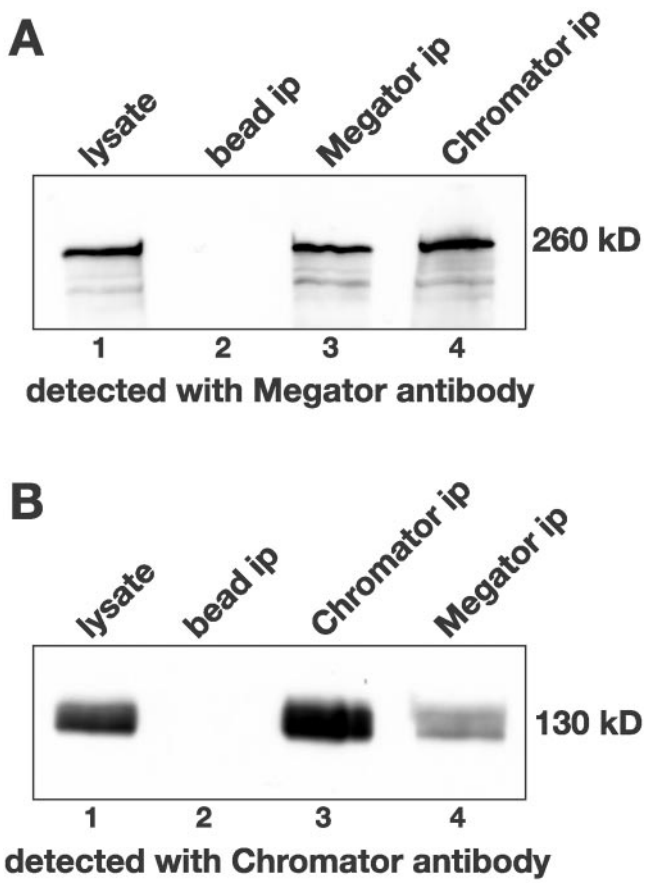

Figure 6. Megator and Chromator immunoprecipitation assays. (A) Immunoprecipitation (ip) of lysates from *Drosophila* embryos were performed using Chromator antibody (mAb 12H9, lane 4) and Megator antibody (mAb 12F10, lane 3) coupled to immunobeads or with immunobeads only as a control (lane 2). The immunoprecipitations were analyzed by SDS-PAGE and Western blotting using Megator mAb 12F10 for detection. Megator antibody staining of embryo lysate is shown in lane 1. Megator is detected in the Megator and Chromator immunoprecipitation samples as a 260-kDa band (lane 3 and 4, respectively) but not in the control sample (lane 2). (B) Immunoprecipitation (ip) of lysates from *Drosophila* embryos were performed using Chromator antibody (mAb 12H9, lane 3) and Megator antibody (mAb 12F10, lane 4) coupled to immunobeads or with immunobeads only as a control (lane 2). The immunoprecipitations were analyzed by SDS-PAGE and Western blotting using Chromator mAb 6H11 for detection. Chromator antibody staining of embryo lysate is shown in lane 1. Chromator is detected in the Megator and Chromator immunoprecipitation samples as a 260-kDa band (lanes 4 and 3, respectively) but not in the control sample (lane 2).

derived Megator protein which masks any potential phenotypes. Furthermore, these animals die before hatching precluding larval neuroblast analysis. For these reasons, we used RNAi methods in S2 cells to deplete Megator protein levels (Figure 8). While we did not observe any obvious perturbation phenotypes of tubulin spindle morphology or chromosome segregation defects by antitubulin and Hoechst labeling of the cells (unpublished data) the number of cells undergoing mitosis was greatly reduced in Megator RNAi treated cultures (Figure 8A). In five separate experiments we determined the mitotic index defined as the number of cells in meta- and anaphase as a percentage of total cell number. Experimental cultures had a mitotic index of 1.8 ± 0.3% (n = 5) vs. an index of 4.3 ± 0.5% (n = 5) in mock treated control cultures representing a reduction of nearly 60% of cells undergoing cell division (Figure 8A). This difference is statistically significant on the $p < 0.0025$ level (Student's *t* test). The degree of Megator knock down in the cultures was determined by immunoblot analysis (Figure 8B) and averaged 86 ± 7% (n = 3) that of mock treated controls. These results suggest that depletion of Megator may prevent cells from entering metaphase.

The COOH-terminal Fragment of Megator Is Sufficient for Nuclear and Spindle Localization

Sequence analysis of Megator identified only one previously known domain, the extended NH_2-terminal coiled-coil domain, in addition to a putative nuclear localization signal (NLS) in the COOH-terminal part. Coiled-coil domains are known to be protein-protein interaction domains that often are involved in self assembly of filamentous structures (Fuchs and Weber, 1994). We therefore tested whether the coiled-coil domain plays a role in the localization of Megator to the putative spindle matrix structure. We made four constructs containing Megator sequences for expression in S2 cells carrying a COOH-terminal V5-tag. The four constructs were a full length Megator construct (Meg-FL), an NH_2-terminal construct (Meg-NT) containing sequence from the starting methionine to residue 1431 that includes 87% of the coiled-coil domain, a COOH-terminal construct (Meg-CT) from residue 1758 to the terminal proline residue containing the putative NLS motif, and a smaller middle construct (Meg-M) from residue 1432–1709. Figure 9 shows examples of expression of these constructs in transiently or stably transfected S2 cells detected with V5-antibody and double-or triple-labeled with lamin or tubulin antibody and Hoechst. The Meg-FL construct localizes to the nucleus (Figure 9A) although its overexpression often leads to aggregation. It is present at the nuclear rim in lamin double labelings at interphase (Figure 9A, top panel) and it is localized to the spindle at metaphase although the distribution is abnormal with aggregation around the spindle poles (Figure 9A, bottom panel, white arrows). The Meg-NT construct containing the coiled-coil domain is not targeted to the nucleus and remains in the cytoplasm typically forming small aggregates (Figure 9B-1). However, in ~30% of transfected S2 cells (n = 320) the Meg-NT construct forms several large spheres outside the nucleus. Three examples of this are shown in Figure 9B. Figure 9B4 shows a maximum projection image from a transfected S2 cell double labeled with Hoechst, whereas Figure 9B5 shows a single confocal section from a different cell demonstrating that the spheres are hollow. Figure 9B6 is a stereo image illustrating the spatial relationship between the spheres. These data suggest that the coiled-coil domain although not targeted to the nucleus nevertheless has the ability to selfassemble into hollow spherical structures. In contrast, the Meg-CT construct is localized to the nucleus, including the nuclear rim at interphase, and colocalizes with the tubulin spindle at metaphase (Figure 9C). Thus the localization of the COOH-terminal Megator construct during the cell cycle phenocopies that of endogenous Megator observed with Megator antibody labeling. This indicates that the coiled-coil domain is not necessary for targeting of Megator to the nucleus but rather that COOH-terminal sequences are sufficient for both nuclear and spindle localization. The Meg-M construct localizes to the cytoplasm, is not present in the nucleus, and does not appear to form aggregates (Figure 9D), suggesting that the behavior of the three other constructs are independent of the V5 tag.

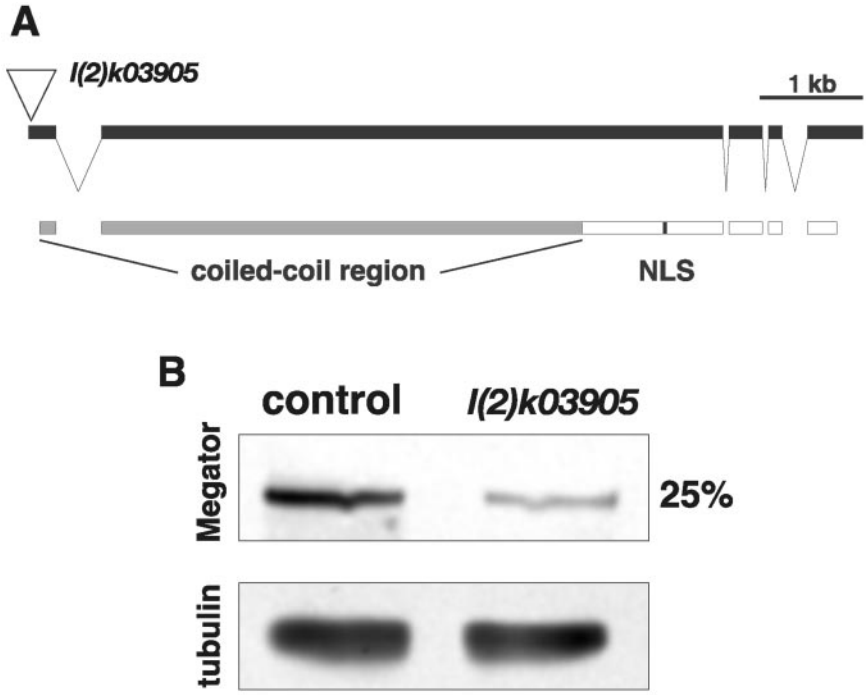

Figure 7. P-element insertion in the *Megator* gene. (A) Diagram of the *Megator* genomic locus. The locus has five exons separated by four introns. The P-element insertion site of line *l(2)k03905* at the +1 position of the Megator cDNA is indicated by the triangle. The ORF coding for the Megator protein including the position of the coiled-coil region and predicted nuclear localization signal (NLS) is depicted underneath. (B) Megator protein expression in homozygous *l(2)k03905* mutant embryos from *l(2)k03905/CyO* parents. The level of Megator expression in *l(2)k03905/CyO* and *CyO/CyO* embryos from the same cross served as a control. The immunoblots were labeled with the anti-Megator Bx34 antibody and with antitubulin antibody. Protein extracts from 35 15–20-h embryos per lane were separated by SDS-PAGE. The relative level of Megator protein expression in mutant embryos as a percentage of Megator expression in control embryos is shown to the right.

DISCUSSION

In this study we show that the Bx34 antigen in addition to the previously reported localization to the extrachromosomal space and nuclear rim at interphase (Zimowska *et al.*, 1997) also interacts with the putative spindle matrix proteins, Skeletor and Chromator, during mitosis. The organization of the Bx34 antigen with a large NH_2-terminal coiled-coil domain and a shorter acidic COOH-terminal domain is similar to the structure of the mammalian Tpr (translocated promoter region) protein (Mitchell and Cooper, 1992) and like Tpr the Bx34 antigen is found at the nuclear rim, likely in association with nuclear pore complexes (Zimowska *et al.*, 1997). However, comparison of Tpr and the Bx34 antigen sequences show a very low level of identity on the amino acid level (Zimowska *et al.*, 1997) and although the Bx34 antigen is abundant in the nuclear interior, mammalian Tpr is restricted to the nuclear periphery (Frosst *et al.*, 2002). Furthermore, mammalian Tpr has not been observed to localize to the spindle at metaphase. Thus, although structurally similar, there is likely to be significant functional differences between the Bx34 antigen and mammalian Tpr, wherefore we have named the Bx34 antigen in *Drosophila*, Megator.

The presence of a large coiled-coil domain in Megator raises the intriguing possibility that it could comprise the structural element of a potential spindle matrix. Because both Chromator and Skeletor localize to chromosomes as well as to the spindle-like structure, it was not clear whether the physical interactions observed in co-ip and pull-down experiments between these molecules reflected interactions in chromosomal complexes or interactions on the spindle-like structure or both (Rath *et al.*, 2004). However, because Megator is not localized to the chromosomes during interphase or on centrosomes during metaphase through telophase, the molecular interaction of the complex observed likely occurs on the spindle-like structure. Interestingly, the Megator deletion construct analysis in S2 cells indicate that the NH_2-terminal coiled-coil containing domain has the abil-

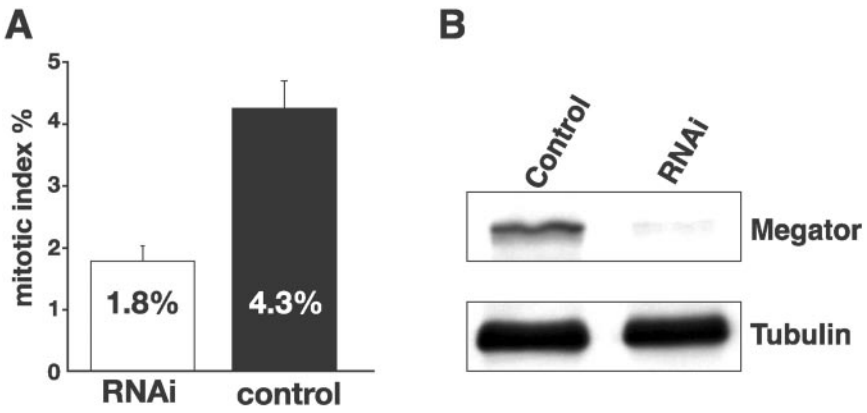

Figure 8. RNAi depletion of Megator in S2 cells leads to a reduction of cells undergoing mitosis. (A) Comparison of the mitotic index of Megator RNAi treated (n = 5) and control (n = 5) S2 cell cultures. The mitotic index was defined as the number of cells in meta- and anaphase as a percentage of total cell number. Megator RNAi treated S2 cell cultures had nearly 60% fewer cells undergoing cell division than mock-treated control cultures. This difference is statistically significant on the $p < 0.0025$ level (Student's *t* test). (B) Western blot with Megator antibody of control-treated and Megator RNAi-treated S2 cells. In the RNAi sample Megator protein level is reduced to ~8% of the level observed in the control cells. Tubulin levels are shown as a loading control.

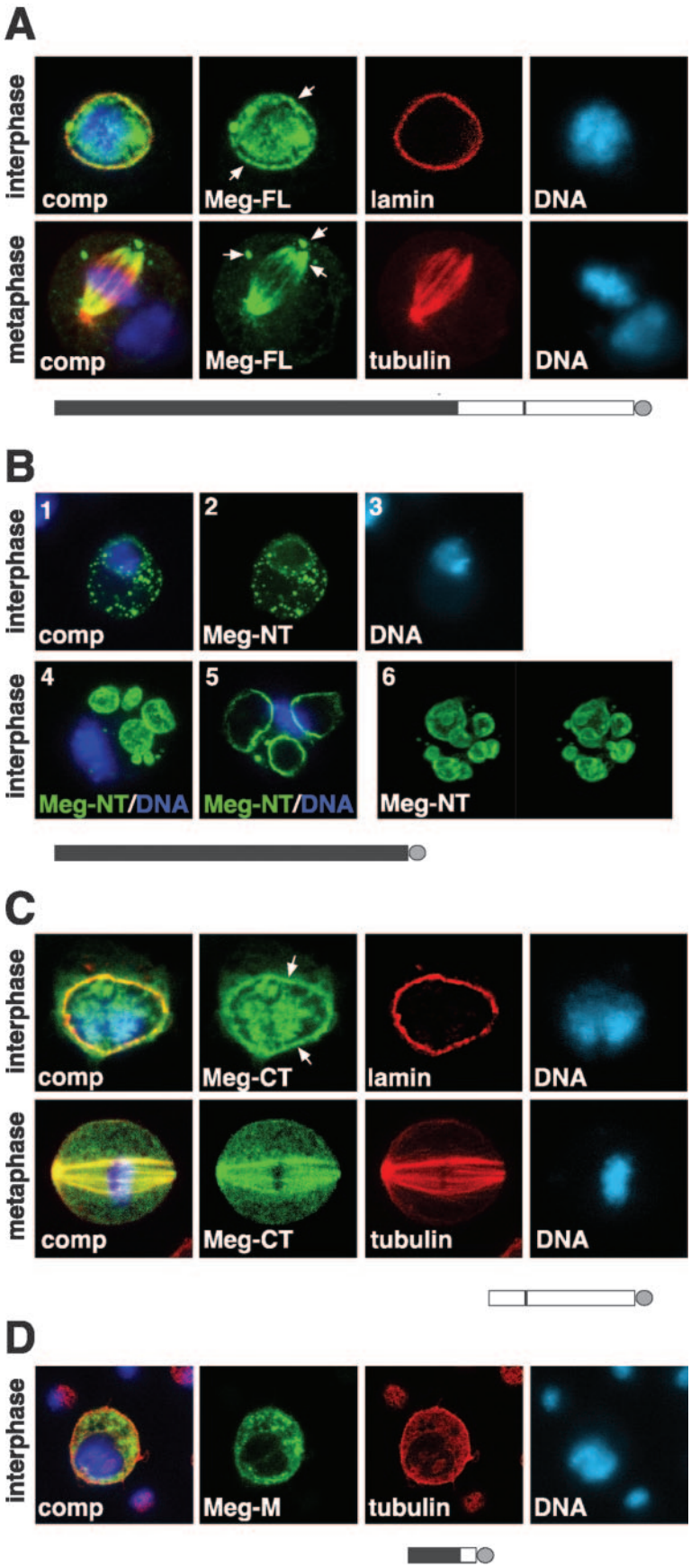

Figure 9. Expression of V5-tagged Megator deletion constructs in S2 cells. The expressed constructs are diagrammed beneath the micrographs. (A) Full-length V5-tagged Megator (Meg-FL) localizes to the nuclear interior and nuclear rim (arrows) of S2 cells at interphase (top panel). The cells were triple-labeled with V5-antibody to visualize the Meg-FL construct (green), lamin antibody (red), and Hoechst to visualize the DNA (blue). The bottom panel shows S2 cells at metaphase labeled with V5-antibody (green), tubulin antibody (red), and Hoechst (DNA in blue). As shown in the composite image (comp) Meg-FL labeling overlaps that of tubulin (yellow color). However, the overexpressed Meg-FL construct also show some aggregation (white arrows). (B) V5-tagged NH_2-terminal Megator deletion construct (Meg-NT) truncated just before the end of the coiled-coil region localizes to the cytoplasm and is mainly absent from the nucleus (top panel). The Meg-NT construct was visualized with V5-antibody (green) and the DNA with Hoechst (blue). In 30% of S2 cells the Meg-NT construct formed several large spheres outside the nucleus (bottom panel). (B4) Maximum projection image from a Meg-NT (green) transfected S2 cell double-labeled with Hoechst (blue). (B5) Single confocal section through a transfected S2 cell demonstrating that the spheres are hollow. (B6) Stereo image of a Meg-NT–transfected cell illustrating the spatial relationship between the spheres. (C) S2 cells at inter- and metaphase expressing a V5-tagged COOH-terminal deletion construct (Meg-CT) lacking the coiled-coil domain. At interphase Meg-CT localizes to the nuclear interior and to the nuclear rim (white arrows). The nucleus was labeled with V5-antibody (green), lamin antibody (red), and the DNA with Hoechst (blue). At metaphase (bottom panel) Meg-CT colocalizes with the microtubule spindle as indicated by the yellow color in the composite image (comp). The cell was labeled with V5-antibody (green), tubulin antibody (red), and the DNA with Hoechst (blue). (D) Interphase labeling in the cytoplasm of an S2 cell expressing the Meg-M construct. The cell was labeled with V5-antibody (green), tubulin antibody (red), and the DNA with Hoechst (blue). All images are from confocal sections. On the diagrams the coiled-coil region is in black, the NLS is indicated by a black bar, and the V5-tag by a gray circle.

ity to selfassemble into spherical structures in the cytoplasm. This is in contrast to the acidic COOH-terminal domain, which is targeted to the nucleus, implying the presence of a functional nuclear localization signal. Furthermore, the COOH-terminal domain is sufficient for localization to the nuclear rim as well as for spindle localization. Thus, an attractive hypothesis is that the COOH-terminal domain functions as a targeting and localization domain, whereas the NH_2-terminal domain may be responsible for forming polymers that may serve as a structural basis for the putative spindle matrix complex. Supporting this notion is the finding that Megator spindles persist in the absence of microtubules depolymerized by cold or nocodazole treatment. The localization of Megator to at least three cellular compartments (nuclear rim, extrachromosomal nuclear space, spindle matrix complex) and reorganization during the cell cycle suggest that it is highly dynamic and that it may exist in several structural forms (Zimowska and Paddy, 2002). This is underscored by the finding that 1 h after heat-shock treatment the amount of Megator protein in the extrachromosomal space diminishes, whereas accumulation occurs at a single chromosomal heat-shock puff, 93D; however, as this occurs Megator localization to the nuclear rim remains unchanged (Zimowska and Paddy, 2002).

The colocalization of Megator with the Skeletor- and Chromator-defined spindle matrix during mitosis suggests that Megator may be involved in spindle matrix function. A spindle matrix has been hypothesized to provide a stationary substrate that anchors molecules during force production and microtubule sliding (Pickett-Heaps *et al.*, 1997). Such a matrix could also be envisioned to have the added properties of helping to organize and stabilize the microtubule spindle (Johansen and Johansen, 2002). Previously, we demonstrated using RNAi assays in S2 cells that depletion of Chromator protein leads to abnormal spindle morphology and that chromosomes are scattered in the spindle, indicating defective spindle function in the absence of Chromator (Rath *et al.*, 2004). However, we are not able to infer a clear functional role for Megator based on the results obtained in the present study. When Megator levels are knocked down by RNAi in S2 cell cultures, the number of cells undergoing mitosis was greatly reduced. However, we did not observe any cells with obvious defects in tubulin spindle morphology or chromosome segregation defects, suggesting that depletion of Megator prevents cells from entering metaphase. This could be due to an essential function of Megator in maintaining nuclear structure and/or in maintaining the integrity of the nuclear rim and pore complexes during interphase or a necessary function for nuclear reorganization during prophase. Thus, if Megator plays multiple functional roles as its dynamic localization pattern suggests (Zimowska and Paddy, 2002), it would prevent us from analyzing a mitotic function using RNAi approaches. That Megator is an essential protein necessary for viability is supported by the embryonic lethality observed as a consequence of P insertions in the *Megator* gene.

Studies using preparations spanning the evolutionary spectrum from lower eukaryotes to vertebrates have provided new and intriguing evidence that a spindle matrix may be a general feature of mitosis (Bloom, 2002; Johansen and Johansen, 2002; Kapoor and Mitchison, 2001). Here we show that at least three proteins, Megator, Chromator, and Skeletor, from two different cellular compartments reorganize to form a putative spindle matrix during mitosis in *Drosophila*. Furthermore, the Megator and Skeletor defined fusiform spindle structure remains intact even in the absence of polymerized microtubules. The identification of several potential spindle matrix molecules in *Drosophila* together with P-element mutations in their genes should provide an avenue for further genetic and biochemical experiments. Especially, the future isolation and characterization of point mutations in *Megator* promises to provide the means to separate Megator's role in spindle matrix function from its role at other stages of the cell cycle.

ACKNOWLEDGMENTS

We thank members of the laboratory for discussion, advice, and critical reading of the manuscript. We also acknowledge V. Lephart for maintenance of fly stocks. We thank L. Ambrosio and the Bloomington Stock Center for generously providing fly stocks and the Developmental Studies Hybridoma Bank at the University of Iowa for providing the lamin antibody. This work was supported by National Science Foundation grant MCB0090877 (K.M.J.) and by Fung and Stadler graduate fellowship awards (D.W., Y.-Z.X., W.Z.).

REFERENCES

Bellotto, M., Bopp, D., Senti, K.-A., Burke, R., Deak, P., Maroy, P., Dickson, B., Basler, K., and Hafen, E. (2002). Maternal-effect loci involved in *Drosophila* oogenesis and embryogenesis: P element-induced mutations on the third chromosome. Int. J. Dev. Biol. *46*, 149–157.

Bloom, K. (2002). Yeast weighs in on the elusive spindle matrix: new filaments in the nucleus. Proc. Natl. Acad. Sci. USA *99*, 4757–4759.

Clemens, J.C., Worby, C.A., Simonson-Leff, N., Muda, M., Maehama, T., Hemmings, B.A., and Dixon, J.E. (2000). Use of double-stranded RNA interference in *Drosophila* cell lines to dissect signal transduction pathways. Proc. Natl. Acad. Sci. USA *97*, 6499–6503.

Frasch, M., Glover, D.M., and Saumweber, H. (1986). Nuclear antigens follow different pathways into daughter nuclei during mitosis in early *Drosophila* embryos. J. Cell Sci. *82*, 155–172.

Frosst, P., Guan, T., Subauste, C., Hahn, K., and Gerace, L. (2002). Tpr is localized within the nuclear basket of the pore complex and has a role in nuclear protein export. J. Cell Biol. *156*, 617–630.

Fuchs, E., and Weber, K. (1994). Intermediate filaments: structure, dynamics, function, and disease. Annu. Rev. Biochem. *63*, 345–382.

Harlow, E., and Lane, E. (1988). Antibodies: A Laboratory Manual, Cold Spring Harbor, NY: Cold Spring Harbor Laboratory Press, 726 pp.

Jin, Y., Wang, Y., Walker, D.L., Dong, H., Conley, C., Johansen, J., and Johansen, K.M. (1999). JIL-1, a novel chromosomal tandem kinase implicated in transcriptional regulation in *Drosophila.* Mol. Cell *4*, 129–135.

Johansen, K.M., and Johansen, J. (2002). Recent glimpses of the elusive spindle matrix. Cell Cycle *1*, 312–314.

Johansen, K.M., and Johansen, J. (2003). Studying nuclear organization in embryos using antibody tools. In: *Drosophila* Cytogenetics Protocols, ed. D.S. Henderson, Totowa, NJ: Humana Press, 215–234.

Johansen, K.M., Johansen, J., Baek, K.-H., and Jin, Y. (1996). Remodeling of nuclear architecture during the cell cycle in *Drosophila* embryos. J. Cell. Biochem. *63*, 268–279.

Kapoor, T.M., and Compton, D.A. (2002). Searching for the middle ground: mechanisms of chromosome alignment during mitosis. J. Cell Biol. *157*, 551–556.

Kapoor, T.M., and Mitchison, T.J. (2001). Eg5 is static in bipolar spindles relative to tubulin: evidence for a static spindle matrix. J. Cell Biol. *154*, 1125–1133.

Klapper, M., Exner, K., Kempf, A., Gehrig, C., Stuurman, N., Fisher, P.A., and Krohne, G. (1997). Assembly of A- and B-type lamins studied in vivo with the baculovirus system. J. Cell Sci. *110*, 2519–2532.

Laemmli, U.K. (1970). Cleavage of structural proteins during assembly of the head of bacteriophage T4. Nature *227*, 680–685.

Mitchell, P.J., and Cooper, C.S. (1992). The human tpr gene encodes a protein of 2094 amino acids that has extensive coiled-coil regions and an acidic C-terminal domain. Oncogene *7*, 2329–2333.

Mitchison, T.J., and Sedat, J. (1983). Localization of antigenic determinants in whole *Drosophila* embryos. Dev. Biol. *99*, 261–264.

Pickett-Heaps, J.D., Tippit, D.H., and Porter, K.R. (1982). Rethinking mitosis. Cell *29*, 729–744.

Pickett-Heaps, J.D., Forer, A., and Spurck, T. (1997). Traction fiber: toward a "tensegral" model of the spindle. Cell Motil. Cytoskeleton *37*, 1–6.

Preston, C.R., and Engels, W.R. (1996). P-element induced male recombination and gene conversion in *Drosophila*. Genetics *144*, 1611–1622.

Rath, U., Wang, D., Ding, Y., Xu, Y.-Z., Qi, H., Blacketer, M.J., Girton, J., Johansen, J., and Johansen, K.M. (2004). Chromator, a novel and essential chromodomain protein interacts directly with the putative spindle matrix protein Skeletor. J. Cell. Biochem. (in press).

Roberts, D.B. (1986). In *Drosophila*: A Practical Approach, Oxford, United Kingdom: IRL Press, 295 pp.

Robertson, H.M., Preston, C.R., Phillis, R.W., Johnson-Schlitz, D.M., Benz, W.K., and Engels, W.R. (1988). A stable genomic source of P element transposase in *Drosophila melanogaster*. Genetics *118*, 461–470.

Sambrook, J., Fritsch, E.F., and Maniatis, T. (1989). Molecular Cloning: A Laboratory Manual, Cold Spring Harbor, NY: Cold Spring Harbor Laboratory Press, 545 pp.

Scholey, J.M., Rogers, G.C., and Sharp, D.J. (2001). Mitosis, microtubules, and the matrix. J. Cell Biol. *154*, 261–266.

Spradling, A.C., Stern, D., Beaton, A., Rhem, E.J., Laverty, T., Mozden, N., Misra, S., and Rubin, G.M. (1999). The Berkeley *Drosophila* Genome Project gene disruption project: single P-element insertions mutating 25% of vital *Drosophila* genes. Genetics *153*, 135–177.

Towbin, H., Staehelin, T., and Gordon, J. (1979). Electrophoretic transfer of proteins from polyacrylamide gels to nitrocellulose sheets: procedure and some applications. Proc. Natl. Acad. Sci. USA *9*, 4350–4354.

Trk, T., Tick, G., Alvarado, M., and Kiss, I. (1993). P-lacW insertional mutagenesis on the second chromosome of *Drosophila melanogaster*: isolation of lethals with different overgrowth phenotypes. Genetics *135*, 71–80.

Walker, D.L., Wang, D., Jin, Y., Rath, U., Wang, Y., Johansen, J., and Johansen, K.M. (2000). Skeletor, a novel chromosomal protein that redistributes during mitosis provides evidence for the formation of a spindle matrix. J. Cell Biol. *151*, 1401–1411.

Wang, Y., Zhang, W., Jin, Y., Johansen, J., and Johansen, K.M. (2001). The JIL-1 tandem kinase mediates histone H3 phosphorylation and is required for maintenance of chromatin structure in *Drosophila*. Cell *105*, 433–443.

Wells, W.A. (2001). Searching for a spindle matrix. J. Cell Biol. *154*, 1102–1104.

Zimowska, G., and Paddy, M.R. (2002). Structures and dynamics of *Drosophila* Tpr inconsistent with a static, filamentous structure. Exp. Cell Res. *276*, 223–232.

Zimowska, G., Aris, J.P., and Paddy, M.R. (1997). A *Drosophila* Tpr protein homolog is localized both in the extrachromosomal channel network and to nuclear pore complexes. J. Cell Sci. *110*, 927–944.

Zink, B., and Paro, R. (1989). In vivo binding pattern of a trans-regulator of homoeotic genes in *Drosophila melanogaster*. Nature *337*, 468–471.